

Modeling and Analysis of SMA-Based Adaptive Structures

Shibin Yang^{1,2} and Stefan Seelecke¹

¹ Department of Mechanical & Aerospace Engineering, North Carolina State University, Raleigh, NC, USA

² Department of Aerospace, Northwestern Polytechnical University, Xi'an, Shaanxi, China
syang5@ncsu.edu, stefan.seelecke@ncsu.edu

Abstract: The application of shape memory alloys (SMA) as actuators in smart structures is a quickly developing field. The particular focus of this paper is on the aspects of modeling and simulation of adaptive structures with integrated SMAs using the finite element method (FEM). A number of generic SMA actuator wire/elastic beam systems are presented first to illustrate the different ways of implementation of SMA models into COMSOL. Finally, a first step towards the simulation of an SMA-based flapping Micro Aerial Vehicle (MAV) is presented. The actuation of a typical bio-inspired humerus-radius system is effected by means of micro-scale actuator wires performing like metal muscles when heated. In addition, the elbow is modeled as a flexible hinge using superelastic SMA wires. This system serves as is the first step towards the design of a flapping wing of a man-made bat, which might propel the next generation MAV. In this bio-inspired bone-joint-system, the humerus and radius were modeled as standard elastic beams. Shape memory alloys were applied in two different ways: one is an SMA wire in the martensite phase, the other is an SMA beam in the austenite phase. The SMA wires function as muscles to actuate the bio-system due to contraction upon electric heating. The SMA beams function as flexible joints due to their superelastic character. In this paper, the modeling and simulation of an active structure, which is actuated by SMAs will be presented.

Keywords: SMA, bone-joint, batwing, active structure

1. Introduction

Smart materials and adaptive structures are now common terms in research and developments. Shape memory alloys, after plastic deformation at low temperature, return to their original shape upon the supply of heat. The material seems to remember its original shape, which gives the name to the effect. SMAs are

applied in two different ways: one is as actuator, the other one makes use of superelasticity. Eyeglass frames and cellular phone antennas are examples of the use of superelasticity, which result in products that are in use worldwide [1]. Various SMA actuators such as wire, compression and tension and cantilever are widely used in electrical and thermal actuation systems [2].

The motivation of this work is to implement SMA materials into bio-inspired micro-aerial-vehicles (MAV). Almost all of the airplanes we can see today use fixed wings, which allow them to fly. The different shape of the wings, camber angles, areas and other characteristics determines the aircraft's aerodynamic performance. Each aircraft was designed for a specific task to fulfill. However, natural flyers hold a big advantage over man-made aircraft in regard to flexibility and efficiency. They are able to fold their wings tightly when they are diving for prey at high speed, or extend their wings completely when they are gliding at low speed. Some birds can fly at very high angles of attack and some insects can even fly sideways or backwards. Birds and insects have a large flight envelope and superior maneuverability because they can change the shape of wings to adapt to different flight conditions. Today this novel technology is called wing morphing [3, 4, 5].

MAVs are a group of Unmanned Aerial Vehicles (UAVs) that are significantly smaller and lighter, with a size of approximately six inches. For such compact scale vehicle, space and mass becomes critical. Compared with traditional actuators, smart materials such as SMA wires have great potential for the actuation of flexible flapping MAVs [6]. In this bio-inspired MAV, the structure is defined by the "bones" of the bird, SMA wires play a role as "muscles" to actuate the wing and a control system is the "brain" of the bird. In this paper, we focus on the modeling and simulation of adaptive structures with integrated SMAs as the first step in this research. The simulation and

analysis of superelastic SMA beams and bio-inspired bone-joint system are also presented.

2. SMAs governing equations

Shape memory alloys exhibit a highly nonlinear and hysteretic constitutive behavior with strong thermo-mechanical coupling. We here introduce the Muller-Achenbach model in the version proposed by Seelecke in more detail [7]. It uses ideas from statistical and thermodynamics and describe the evolution of two martensite fractions based on the theory of thermally activated processes.

The stress-strain relation can be expressed as

$$\sigma(\varepsilon) = \frac{E_M [\varepsilon - (x_+ - x_-) \varepsilon_T]}{x_+ + x_- + \frac{E_M}{E_A} x_A} \quad (1)$$

The evolution of the phase fractions x_α ($\alpha = A, +, -$) is governed by the rate laws

$$\begin{aligned} \dot{x}_+ &= -x_+ p^{+A} + x_A p^{A+} \\ \dot{x}_- &= -x_- p^{-A} + x_A p^{A-} \end{aligned} \quad (2)$$

The phase fraction of austenite x_A is given as

$$x_A = 1 - x_+ - x_- \quad (3)$$

The quantities $p^{\alpha\beta}$ are called transition probabilities. Transition probabilities are computed as the product of the probability of achieving the energy required to overcome the energy barrier and the frequency at which jumps are tempted [7].

SMA actuators are typically driven by joule heating and convective cooling. Assuming uniform temperature changes throughout the SMA material, the heat transfer equation reads [7]

$$\rho c \dot{T} = -\alpha S_V (T - T_0) + j(t) - (h_{M_+} - h_A) \dot{x}_+ - (h_{M_-} - h_A) \dot{x}_- \quad (4)$$

T is temperature. The terms $h_{M_\pm} - h_A$ are called the latent heat of the transformations, ρ is the density and c is the specific heat. A(x) is the cross section area, σ is stress. $j(t)$ is joule heating as the input of the SMA wire actuator.

Equation (2) and (3) are ODEs, which for the COMSOL implementation, we interpret as degenerate PDEs without flux term. Hence, the SMA wire can be modeled as a 1-D general PDE mode application in COMSOL [8, 9].

The governing equations are:

$$d_\alpha \frac{\partial U}{\partial t} + \frac{\partial \Gamma}{\partial x} = F \quad (5)$$

$$U = [u \quad x_+ \quad x_- \quad T]^T \quad (6)$$

where u is displacement.

$$d_\alpha = \begin{bmatrix} 0 & 0 & 0 & 0 \\ 0 & 1 & 0 & 0 \\ 0 & 0 & 1 & 0 \\ 0 & (h_{M_+} - h_A) & (h_{M_-} - h_A) & \rho c \end{bmatrix} \quad (7)$$

$$\Gamma = \begin{bmatrix} A(x)\sigma(x) \\ 0 \\ 0 \\ 0 \end{bmatrix} \quad (8)$$

$$F = \begin{bmatrix} 0 \\ -x_+ p^{+A}(\sigma, T) + (1 - x_+ - x_-) p^{A+}(\sigma, T) \\ -x_- p^{-A}(\sigma, T) + (1 - x_+ - x_-) p^{A-}(\sigma, T) \\ -\alpha \frac{l_c(x)}{A(x)} (T - T_0) + j(t) \end{bmatrix} \quad (9)$$

The first equation for variable “u” is the mechanical equilibrium, neglecting the inertia of the wire. The corresponding boundary conditions are

Dirichlet condition at x=0:

$$r_1 = hu + b = 0 : u(0, t) = 0 \Rightarrow r_1 = u \quad (10)$$

Neumann condition at x=L:

$$-n \cdot \Gamma = g_1 : A(L)\sigma(L, t) = F(t) \Rightarrow g_1 = F(t) \quad (11)$$

There is no restriction on the phase fractions at both ends, so boundary conditions for x_α are implemented as $r_\alpha = 0$. The last equation is the energy balance along the SMA wire, which enables us to calculate the temperature field in response to electric power input; for details and relevance of such analysis see [8].

3. Integration of structures and SMA actuators

To illustrate the simulation of an adaptive structure with SMA actuators, an adaptive beam actuated by one SMA actuators was modeled. The system is comprised of a SMA wire mounted to stiff rectangular standoff stubs, which are mounted to a flexible beam (Figure 1). Material properties and dimensions are shown in the Table 1. The flexible beam is represented by a typical thermoplastic material, and the SMA stubs are composed of aluminum. In the sequel we will introduce two ways to implement the SMA model in the simulation.

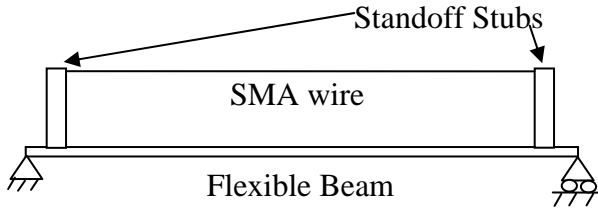


Figure 1 Adaptive beam actuated by one SMA wire

Table 1 Material properties and dimensions

| Flexible Beam | | Units |
|----------------|-------|-------|
| Youngs modulus | 2.756 | GPa |
| Length | 85 | mm |
| Width | 20 | mm |
| Height | 1 | mm |
| Standoff Stubs | | |
| Youngs modulus | 70 | Gpa |
| Length | 10 | mm |
| Width | 2.5 | mm |
| Height | 2.5 | mm |
| SMA Actuators | | |
| Length | 75 | mm |
| Diameter | 0.05 | mm |

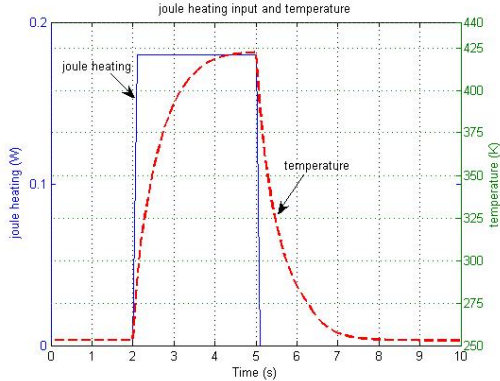


Figure 2 Joule heating input and temperature at the wire midpoint

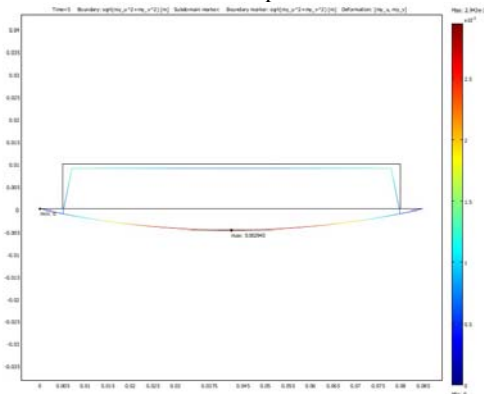


Figure 3 Deformation at 5s

3.1 Periodic boundary conditions

In order to integrate SMA wires into the conventional structures, the first method uses periodic boundary conditions. Periodic boundary conditions define a constraint that makes two quantities equal on two different domains. COMSOL Multiphysics implements a periodic boundary condition as a special case of the extrusion coupling variable [9]. Below are the implementation steps.

Step 1: Model 1-D SMA wire in PDE general form as introduced in Section 2.

Step 2: Model the adaptive structure in a new geometry. The flexible beam and standoff stubs are modeled as 2-D In-Plane Euler beams. The line which represents the SMA wire is modeled as a truss with zero Young's modulus. This ensures the truss only provides an additional constraint such that the deformation is in the direction of the truss while not influencing the stiffness of the whole structure.

Step 3: Add the SMA wire model as a component to the structural model. Since they are different dimensions, they will be shown in 2 geometries.

Step 4: Specify the periodic boundary conditions in order to couple the truss and SMA wire in different geometries. Specify the same expression "u" to them, one is source, the other is destination. The truss will thus be overwritten by the SMA wire.

Joule heating and temperature history at the wire midpoint are given in Figure 2. Figure 3 shows the deformation of the adaptive structure at t=5s.

3.2 Self-defined coupling variables

When the focus of the analysis is on the global structural response, it is not necessary to calculate the details of the temperature and strain field along the wire. Under the assumption of homogenous temperature throughout SMA materials, the strain and stress as well as phase fractions are all homogenous along the wire. As a result, the first equation in (5), which describes inertia, can be deleted. When joule heating is applied to the SMA actuator, it will have a tendency to contract and exert forces on the structure. The structure will deform under the forces and give constraints back to the SMA wire. As a result, variables " \mathcal{E} " and " F " are involved to couple the structure and the SMA wire, which is now represented by only one

element that we model using the ODE option. The implementation procedure is:

Step 1: Model 1-D SMA wire based on section 2 without variable “u”.

Step 2 and **Step 3** are the same as section 3.1.

Step 4: Add algebraic equation for SMA wire strain :

$$\varepsilon = \frac{L(t) - L_0}{L_0} \quad (12)$$

where $L(t)$ is the distance between the two SMA wire attachment points which can be obtained from the deformation of the structure.

L_0 is the original length of the SMA wire.

Step 5: Add algebraic equation for reaction force

$$F = \sigma \cdot A(x) \quad (13)$$

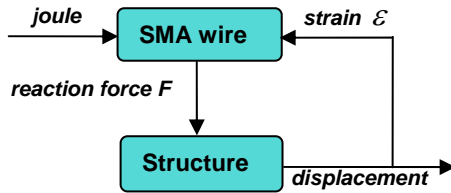


Figure 4 Flow chart for adaptive beam simulation

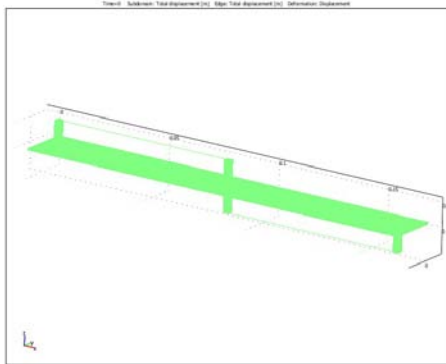


Figure 5 3-D adaptive beam and 2 SMA wires

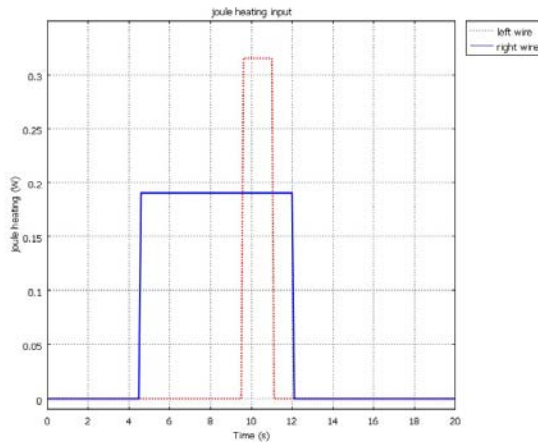


Figure 6 Joule heating input

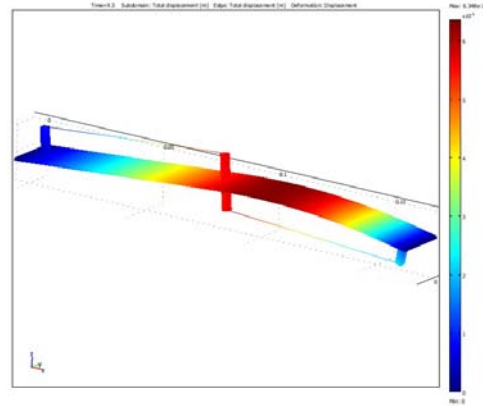


Figure 7 Deformation at 9.5s

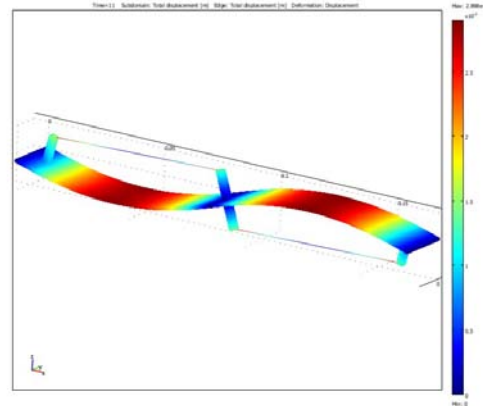


Figure 8 Deformation at t=11s

Variables “ ε ” and “ F ” are defined as global variables, so as to be used in different geometries. Figure 4 gives the simulation flow chart. The structure communicates the strain to the SMA wire, and SMA wire communicates the forces back to the structure. This coupling approach is simpler and computationally more efficient than the one in Section 3.1 and yields the same results if the details of the actuator are not of prime interest. Figure 5 shows a 3-D adaptive beam, which is actuated by 2 SMA wires. This simulation approximately replicates a lab experiment carried out in [10] and the simulation in ANSYS reported in [11]. The joule heating inputs are illustrated in Figure 6. Figure 7 and Figure 8 are the deformation of the adaptive structure at different time.

4. Analysis of superelastic SMA beam

Together with the small deformation Euler-Bernoulli beam theory, a SMA beam is treated as consisting of several layers. So the 1-D SMA model described in Section 2 can be applied to each layer to model the beam bending problem [8, 12].

For the cantilever beam, the force equilibrium equation can be derived as

$$\frac{\partial Q}{\partial x} = -q(x) \quad (14)$$

and the moment equilibrium yields the following relation between the shear force $Q(x)$ and the cross-section moment $M(x)$

$$\frac{\partial M}{\partial x} = Q \quad (15)$$

The stress-strain relation is the same as for the SMA wire except for the function of position y .

$$\sigma(x, y) = \frac{E_M [\varepsilon(x, y) - (x_+ - x_-) \varepsilon_T]}{x_+ + x_- + \frac{E_M}{E_A} x_A} \quad (16)$$

From the kinematic assumptions of the Euler-Bernoulli Beam theory, the strain is calculated as

$$\varepsilon(x, y) = -y \frac{\partial \theta}{\partial x} \quad (17)$$

with the deflection angle $\theta(x)$ following from the transverse deflection $W(x)$ of the beam as

$$\frac{\partial W}{\partial x} = \theta \quad (18)$$

The cross-section moment can be approximated using Gauss integration as

$$\begin{aligned} M(x) &= b \int_{-h/2}^{h/2} y \sigma(x, y) dy \\ &= \frac{bh^2}{4} \int_{-1}^1 \xi \sigma(x, \xi) d\xi \quad (y = \frac{h}{2} \xi) \\ &= \frac{bh^2}{4} \sum_{i=1}^n w_i \xi_i \sigma(x, \frac{h}{2} \xi_i) \end{aligned} \quad (19)$$

where ξ_i and w_i Gauss integration points and corresponding weights, respectively. The index i refers to the i th layer.

The cross-section moment can be expressed as an affine function of the curvature of the neutral axis $\frac{\partial \theta}{\partial x}$ as

$$M(x) = \beta \frac{\partial \theta}{\partial x} + \gamma \quad (20)$$

where the expressions for β and γ can be found in detail in [8].

Using the shear force Q , moment M , deflection angle θ , deflection W and phase fractions $x_+^i, x_-^i (i=1, \dots, n)$ as solution variables $U = [Q \ M \ \theta \ W \ x_+^1 \ x_-^1 \ \dots \ x_+^n \ x_-^n]^T$ we can write the problem again as a degenerate PDE system. Each layer refers to a pair of phase fractions. They have the same expressions as the

SMA wire in Section 2. Then, the quasi-static bending problem of the SMA cantilever beam can be implemented in the COMSOL general form PDEs as

$$d_\alpha \frac{\partial U}{\partial t} + \frac{\partial \Gamma}{\partial x} = F \quad (21)$$

In this section, moment and force applied to the SMA cantilever are presented separately. The effects of number of elements and layers are studied.

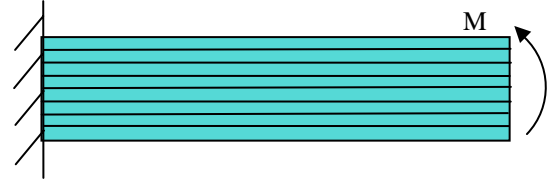


Figure 9 Superelastic SMA cantilever beam modeled as multi-layers structure

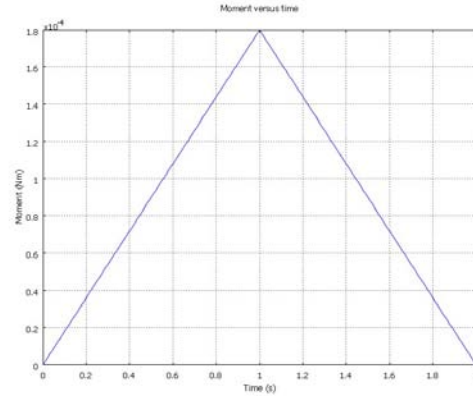


Figure 10 Moment input

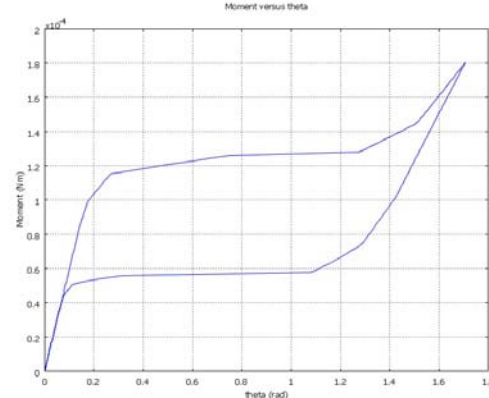


Figure 11 Moment vs. rotation angle

First, we consider a superelastic SMA cantilever, to which a time-dependent moment is applied at the right endpoint while the left endpoint is clamped (Figure 9). Figure 10 and Figure 11 demonstrate the Moment input and Moment vs. deflection at right endpoint separately. Studying the effect of element number for a fixed number of layers, we find that increasing the number of elements does not improve the accuracy in this simulation. That is

because the moment is homogenous along the beam. It means that the stress and strain as well as phase fractions are the same in one layer at any given time step. As a result, we can model the joint with just one element. However, there are differences between the different layers. Since there is no analytical solution for such problem, here, we studied the convergence behavior for varying layer numbers. Figure 12 shows the result of moment versus rotation angle for different layer numbers. Increasing the number of layers, we find the solution to converge, and we can see that the result of 8 layers is very close to the one of 10 layers. Finally, we choose a superelastic SMA beam model of 1 element, 8 layers.

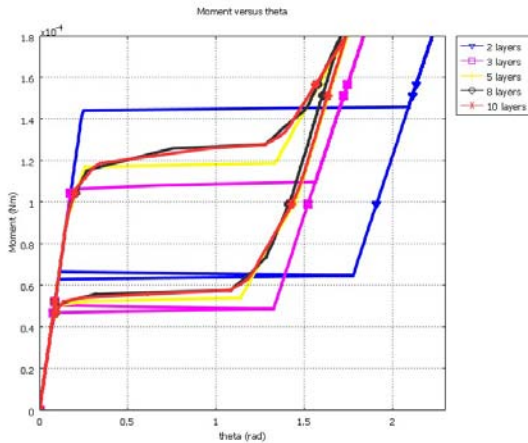


Figure 12 Moment vs. rotation angle (different layers)



Figure 13 Superelastic SMA cantilever force applied

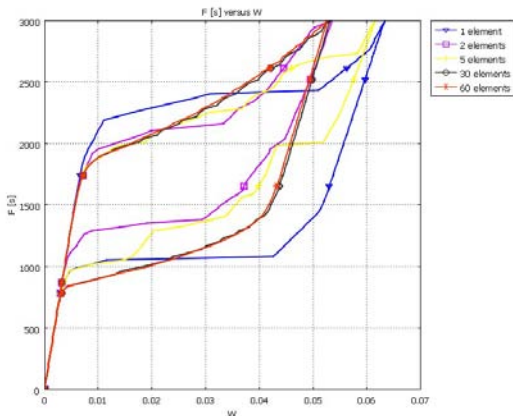


Figure 13 Superelastic SMA cantilever force applied

For force applied to the superelastic SMA cantilever problem (Figure 13), the variables are not homogenous along the beam any more. For certain layers, the more elements it has, the better result it will achieve. We can see from Figure 14, the result of 30 elements is close to one with 60 elements. More elements can get smoother results.

5. Bone-joint system

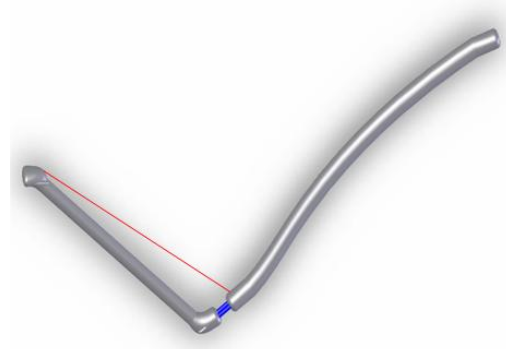


Figure 15 Bio-inspired bone-joint system model with SMA wire actuation (red) and superelastic joint (blue)

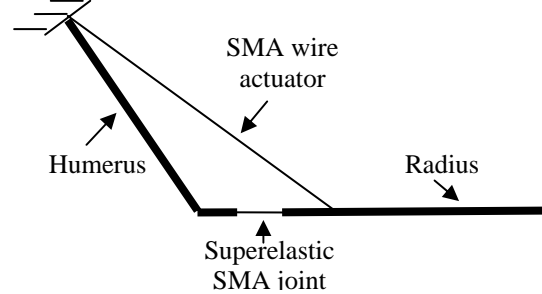


Figure 16 Geometry model of the bone-joint system

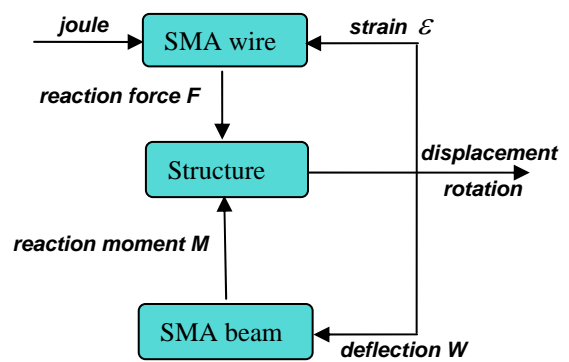


Figure 17 Simulation flow chart

Figure 15 shows the engineering model of a bat's humerus, elbow and radius. Here, we model this bio-inspired bone-joint system as 2D Euler beams in COMSOL, see Figure 16. The superelastic SMA beam is located between two bones as a joint. The length of the SMA beam L is 1mm, the diameter d is $100 \mu m$. The SMA

actuator wire links the left endpoint of the “humerus” and an inner point on “radius”. The distance between attachment point and the left endpoint of the “radius” is 1mm. The length of the SMA actuator wire is L is 24.4mm.

Figure 17 illustrated the simulation flow chart of the bone-joint system. When we apply joule heating to the pre-strained SMA wire, it will transform from martensite $M+$ to austenite A , which results in a contraction of the SMA wire. At the same time, the superelastic SMA beam will be bent under the reaction moment from the “radius”. The “radius” will be rotated under the force from the SMA wire and the constraint from the joint. Upon convective cooling and under tensile stress, the SMA wire transforms from A back to $M+$ and returns to the original length. The joint and the bones also return to their original position. This work is trying to integrate the traditional structure, SMA actuators and SMA beam joint together. In COMSOL, these components are modeled in three geometries, and are coupled via reaction forces, reaction moment and constraints. In structure geometry, the SMA wire is defined as truss with zero Young’s modulus; the superelastic SMA beam is defined as 2D beam with zero Young’s modulus and $I_{yy} = 0$. Under the homogeneous assumption, the reaction force can be expressed as

$$F = \sigma \cdot A \quad (22)$$

The reaction moment can be expressed as:

$$M = f(W) \quad (23)$$

where W is the deflection of the right point of SMA beam. The obvious benefit is modularization. We can add multi SMA wires and superelastic joints as we want.

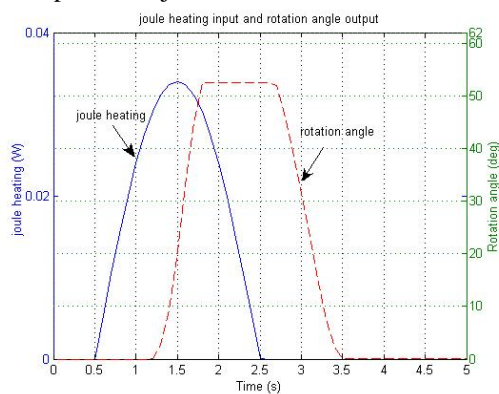


Figure 18 Joule heating (red dash) and radius rotation angle (blue solid)

Figure 18 gives the joule heating input to the SMA actuator wire and radius rotation angle. It is a sine function with a period of 0.5s~2.5s. The

amplitude is 0.034W. We can see that it has a delay and nonlinearities.

6. Conclusions

Shape memory alloys are a very promising material for quasistatic or low bandwidth applications, in particular where high work output per volume is needed. This article introduced one of the shape memory alloy applications in the field of adaptive structure: the flapping micro aerial vehicle. The bio-inspired batwing was chosen because it has suitable mass and wing beat frequency. Shape memory alloys have strongly nonlinear and hysteretic dynamic behaviors under coupled thermodynamic and mechanical situations. Previously, shape memory alloys have been simulated accounting their particular characters. Unlike traditional structures, the adaptive smart structures actuated by smart materials have to be studied and designed in a coupling way. The present work focuses on development and analysis of a finite element coupled model which contains shape memory alloys and traditional structures. In the next step, the model will be extended to 3D, and the SMA wire’s attachment position will be studied. In order to allow the joint to bend in a plane, two superelastic SMA beams might be necessary. Furthermore, a suitable optimal control algorithm should be studied in the future.

7. References

- [1] Ming H. Wu and L. McD. Schetky, Industrial Applications for Shape Memory Alloys, Proceedings of the International Conference on Shape Memory and Superelastic Technologies, Pacific Grove, California, P.171-182 (2000).
- [2] D. Stockel, The martensitic Transformation in Science and Technology, ed., E. Hornbogen and N. Jost, Informationsgesellschaft-Verlag, p.223, 1989.
- [3] Kudva, J. N., Overview of the DARPA/AFRL/NASA smart materials and structures and Smart Wing program, Proceedings of SPIE, Vol. 4698, San Diego, 18-21 March 2002
- [4] Martin, C. A., Design, fabrication, and testing of scaled wind tunnel model for the Smart Wing Phase 2 program, Proceedings of SPIE, Vol. 4698, San Diego, 18-21 March 2002
- [5] Brian Sanders, Dave Cowan and Lewes Scherer, Aerodynamic Performance of the Smart

Wing Control Effectors, Journal of Intelligent Material Systems and Structures, Vol. 15, 2004

[6] Gheorghe Bunget, BATWING: A Biologically-Inspired Micro-Air Vehicle for Flapping Flight – Kinematic Modeling, Master thesis, North Carolina State University, Department of Mechanical Engineering, Raleigh, 2007

[7] Stefan Seelecke, Ingo Muller, Shape memory alloy actuators in smart structures: Modeling and simulation, ASME Applied Mechanics Reviews, 57, pp.23-46, 2004.

[8] Qifu Li, Modeling and Finite Element Analysis of Smart Materials, PhD thesis, North Carolina State University, Department of Mechanical Engineering, Raleigh, 2006

[9] COMSOL help documentation, COMSOL Inc.

[10] S. Seelecke, Control of Beam Structures by Shape Memory Wires, Proceedings of the 2nd Sci. Conf. Smart Mechanical Systems Adaptronics, Otto-von-Guericke Univ. Magdeburg, 1997

[11] Jason Paul Frautschi, Finite Element Simulations of Shape Memory Alloy Actuators in Adaptive Structures, Master thesis, NC State University, Department of Mechanical and Aerospace Engineering, Raleigh, 2003

[12] Qifu Li, Stefan Seelecke, M. Kohl and B. Krevet, Thermo-mechanical Finite Element Analysis of a Shape Memory Alloy Cantilever Beam, SPIE06-6166-73.